Random vibration of multispan Timoshenko frames due to a moving load

Rong-Tyai Wang †

Department of Engineering Science, National Cheng Kung University, Tainan, Taiwan, R.O.C.

Jin-Sheng Lin ‡

Housing and Urban Development Bureau, Taiwan, R.O.C.

Abstract. In this paper, an analytic method to examine the random vibration of multispan Timoshenko frames due to a concentrated load traversing at a constant velocity is presented. A load's magnitude is a stationary process in time with a constant mean value and a variance. Two types of variances of this load are considered: white noise process and cosine process. The effects of both velocity and statistical characteristics of load and span number of the frame on both the mean value and variance of deflection and moment of the structure are investigated. Results obtained from a multispan Timoshenko frame are compared with those of a multispan Bernoulli-Euler frame.

Key words: Timoshenko frames; random vibration; load; velocity; span number.

1. Introduction

The problem of loads moving on structures has been studied for many years (Dmitriev 1982, Blejwas *et al.* 1979, Fry'ba 1971, Mackertich 1990, Wang and Lin 1997b). In modern cities, guideways and elevated bridges are becoming increasingly important transportation systems. Guideways and elevated bridges have similar frame structures. The dynamic deflection of multispan frames due to a constant moving load is greater than that induced by the same load in a static situation. Furthermore, a moving load's velocity is the dominant factor on the frames' vibration. Due to the technological progress, the speed and weight of vehicles have become more complex than ever. In actual situations, magnitude and velocity of moving loads cannot be described deterministically. Consequently, the frames' responses cannot be obtained exactly. Fortunately, the stochastic characteristics of traffic flows can be estimated. The frames' random vibration owing to moving loads such as traffic flows will induce the structures' fatigue. Therefore, this kind of random vibration is a relevant topic in structural dynamics.

Simple beams are generally taken as examples to study a structure's random vibration due to moving loads (Bolotin 1984, Fry'ba 1976, Iwankiewicz and Sniady 1984, Knowles 1968, Sniady 1984, Ricciardi 1994). The type of a multispan frame is different from a simple beam.

† Professor
‡ Former Graduate Student

A multispan frame's vibration can be analyzed by the finite element method (FEM). However, the FEM is not feasible for studying the problem of moving loads on a multispan frame (Wang and Lee 1993). Wang and Lin (1997a) successfully demonstrated the modal analysis method while studying the vibration of a multispan Bernoulli-Euler frame due to a constant moving load. In this study, the approach of modal analysis is presented to investigate the multispan Timoshenko frames' random vibration due to a moving load.

The Bernoulli-Euler beam model is normally used in structural analysis. This model may bring about erroneous results in a dynamic situation (Clough 1955). The Timoshenko beam model is then proposed to correct errors due to the Bernoulli-Euler beam model (Timoshenko 1921). In addition to shear deformation and rotatory inertia, the axial deformation is included for examining the vibration of T-type Timoshenko frames (Wang and Lin 1997b). In this study, the model of multispan Timoshenko frames is considered to study the random vibration of frame due to a moving load. A frame's material is homogeneous and isotropic with Young's modulus E, shear modulus G, Poisson's ratio μ and mass density ρ. A frame's geometry has a cross-sectional area A, second moment of area I, radius of gyration of cross section η and shear coefficient κ. Each frame's beam has an equal length L. Moreover, the length L^* is the same for each column. A concentrated load moving on a multispan frame at a constant velocity is taken as an example to investigate the stochastic characteristics of deflection and moment of the structure. A load's magnitude is proposed to be a stationary process in time with a constant mean value and a variance. Two processes of variances are treated as examples: a white noise process and a cosine process. The velocity effect of load and the span number effect on the mean value of responses of the frame are examined. Furthermore, the velocity effect and the variance type on the standard deviation of responses are also studied. Moreover, results of a multispan Timoshenko frame are compared with those of a multispan Bernoulli-Euler frame.

2. Governing equations

Fig.1 depicts a distributed load $F(x, t)$ on an n-span Timoshenko frame. The longitudinal displacement, transverse displacement, rotatory angle, axial force, transverse shear force and bending moment of the ith beam component of the frame are respectively denoted as u_i, w_i, ψ_i, n_i, q_i and m_i which are

$$n_i = EA\frac{\partial u_i}{\partial x}, \quad q_i = \kappa GA\left(\frac{\partial w_i}{\partial x} - \psi_i\right), \quad m_i = -EI\frac{\partial \psi_i}{\partial x} \tag{1}$$

where x is the axial coordinate. The equations of motion of the beam are
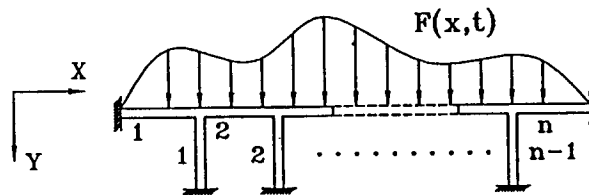

Fig. 1 A distributed load $F_{(x, t)}$ on an n-span Timoshenko frame

$$\frac{\partial n_i}{\partial x} = \rho A \frac{\partial^2 u_i}{\partial t^2} \tag{2a}$$

$$\frac{\partial q_i}{\partial x} + F_i(x, t) = \rho A \frac{\partial^2 w_i}{\partial t^2} \tag{2b}$$

$$q_i - \frac{\partial m_i}{\partial x} = \rho I \frac{\partial^2 \psi_i}{\partial t^2} \tag{2c}$$

where t is time and $F_i(x, t)$ is the component of load on the beam. The sign convention for displacements and applied forces at both ends of the beam (see Fig. 2) are

$$\{u \ w \ \psi n \ q \ m\}_{ia} = \{u \ w \ \psi - n \ -q \ m\}_i \ |_{x=(i-1)L},$$
$$\{u \ w \ \psi n \ q \ m\}_{ib} = \{u \ w \ \psi n \ -q \ m\}_i \ |_{x=iL}, \tag{3}$$

The equations of motion of the ith column of the frame are

$$\frac{\partial n_i^*}{\partial x_i} = \rho A \frac{\partial^2 u_i^*}{\partial x_i^2} \tag{4a}$$

$$\frac{\partial q_i^*}{\partial x_i} = \rho A \frac{\partial^2 w_i^*}{\partial t^2} \tag{4b}$$

$$q_i - \frac{\partial m_i^*}{\partial x} = \rho I \frac{\partial^2 \psi_i^*}{\partial t^2}, \qquad i = 1, 2, \cdots, n-1 \tag{4c}$$
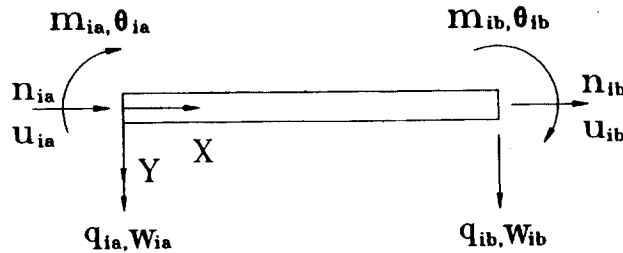

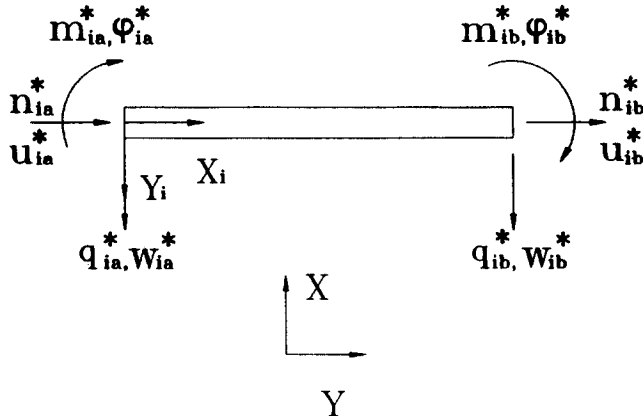Fig. 2 Applied end forces and displacements of the ith beam

Fig. 3 Applied end forces and displacements of the ith column

where $u_i{}^*$, $w_i{}^*$, $\psi_i{}^*$, $n_i{}^*$, $q_i{}^*$ $m_i{}^*$ and x_i are the longitudinal displacement, transverse displacement, rotatory angle, axial force, transverse shear force, bending moment and axial coordinate of the column, respectively. Moreover, the sign convention of displacements and applied forces at both ends of the column (see Fig. 3) is

$$\{u \ w \ \psi n \ q \ m\}_{ia}^* = \{u \ w \ \psi - n - q \ m\}_i^* \mid_{x_i = 0},$$

$$\{u \ w \ \psi n \ q \ m\}_{ib}^* = \{u \ w \ \psi n - q \ m\}_i^* \mid_{x_i = L^*} \tag{5}$$

The displacement conditions at the fixed ends of the frame are

$$u_{1a} = u_{nb} = 0, \qquad w_{1a} = w_{nb} = 0, \qquad \psi_{1a} = \psi_{nb} = 0 \tag{6a}$$

$$u_{ib}^* = 0; \ w_{ib}^* = 0; \ \psi_{ib}^* = 0, \qquad i = 1, 2, \cdots, n - 1 \tag{6b}$$

Moreover, the displacements continuity and the forces balance at the ith junction of the ith column and two connected beams are

$$\psi_{ib} = \psi_{(i+1)a} = \psi_{ia}^*; \ u_{ib} = u_{(i+1)a} = -w_{ia}^*; \ w_{ib} = w_{(i+1)a} = u_{ia}^* \tag{6c}$$

$$m_{ib} + m_{(i+1)a} + m_{ia}^* = 0, \ q_{ib} + q_{(i+1)a} + n_{ia}^* = 0, \ n_{ib} + n_{(i+1)a} - q_{ia}^* = 0 \tag{6d}$$

Eqs. (1)-(6d) constitute the governing equations of the frame structure.

3. Modal frequencies

To calculate the modal frequencies of the frame, the longitudinal displacement u_i, transverse deflection ψ_i, rotatory angle ψ_i, axial force n_i, shear force q_i and bending moment m_i of the ith beam are expressed as

$$\{u \ w \ \psi n \ q \ m\}_i (x, t) = \{U \ W \ \Psi N \ Q \ M\}_i (x) \sin(\omega t), \ (i-1)L \leq x \leq iL \tag{7}$$

in which ω is the circular frequency and the function $U_i(x)$ is (Wang and Lin 1997b)

$$U_i(x) = B_{1i} \cos(\lambda x) + B_{2i} \sin(\lambda x) \tag{8}$$

where $\lambda = (\rho/E)^{1/2} \omega$, B_{1i} and B_{2i} are two constants. Moreover, the functions W and Ψ are (Wang and Lin 1997b)

case 1. for $\lambda^2 < \dfrac{\kappa}{2(1+\mu)\eta^2}$

$$W_i(x) = B_{3i} \cosh(p_1 x) + B_{4i} \sinh(p_1 x) + B_{5i} \cos(p_2 x) + B_{6i} \sin(p_2 x) \tag{9a}$$

$$\Psi_i(x) = \beta_1(p_1)[B_{4i} \cosh(p_1 x) + B_{3i} \sinh(p_1 x)]$$
$$+ \beta_2(p_2)[B_{5i} \sinh(p_2 x) - B_{6i} \cosh(p_2 x)] \tag{9b}$$

where

$$p_1^2 = -\frac{\lambda^2}{2}\left[1 + \frac{2(1+\mu)}{\kappa}\right] + \left\{\frac{\lambda^4}{4}\left[1 + \frac{2(1+\mu)}{\kappa}\right]^2 + \left[\frac{\lambda^2}{\eta^2} - \frac{2(1+\mu)\lambda^4}{\kappa}\right]\right\}^{1/2}$$

$$p_2^2 = -\frac{\lambda^2}{2}\left[1+\frac{2(1+\mu)}{\kappa}\right] + \left\{\frac{\lambda^4}{4}\left[1+\frac{2(1+\mu)}{\kappa}\right]^2 + \left[\frac{\lambda^2}{\eta^2}-\frac{2(1+\mu)\lambda^4}{\kappa}\right]\right\}^{1/2}$$

$$\beta_1(p) = \frac{1}{p}\left[p^2+\frac{2(1+\mu)\lambda^2}{\kappa}\right]; \beta_2(p) = \frac{1}{p}\left[-p^2+\frac{2(1+\mu)\lambda^2}{\kappa}\right],$$

or

case 2. for $\lambda^2 > \dfrac{\kappa}{2(1+\mu)\eta^2}$

$$W_i(x) = B_{3i}\cos(p_1 x) + B_{4i}\sin(p_1 x) + B_{5i}\cos(p_2 x) + B_{6i}\sin(p_2 x) \tag{9c}$$

$$\Psi_i(x) = \beta_2(p_1)[-B_{4i}\cos(p_1 x) + B_{3i}\sin(p_1 x)]$$
$$+ \beta_2(p_2)[B_{5i}\sin(p_2 x) - B_{6i}\cos(p_2 x)] \tag{9d}$$

where

$$p_1^2 = \frac{\lambda^2}{2}\left[1+\frac{2(1+\mu)}{\kappa}\right] - \left\{\frac{\lambda^4}{4}\left[1+\frac{2(1+\mu)}{\kappa}\right]^2 + \left[\frac{\lambda^2}{\eta^2}-\frac{2(1+\mu)\lambda^4}{\kappa}\right]\right\}^{1/2}$$

$$p_2^2 = \frac{\lambda^2}{2}\left[1+\frac{2(1+\mu)}{\kappa}\right] + \left\{\frac{\lambda^4}{4}\left[1+\frac{2(1+\mu)}{\kappa}\right]^2 + \left[\frac{\lambda^2}{\eta^2}-\frac{2(1+\mu)\lambda^4}{\kappa}\right]\right\}^{1/2}$$

$$\beta_2(p) = \frac{1}{p}\left[-p^2+\frac{2(1+\mu)\lambda^2}{\kappa}\right]$$

Substituting Eqs. (8)-(9d) into Eq. (1) yields the corresponding axial force $N_i(x)$, transverse shear force $Q_i(x)$ and moment $M_i(x)$. The constants B_{1i} - B_{6i} of Eqs. (8)-(9d) are determined by the boundary conditions of the ith beam.

Similarly, the axial displacement, transverse deflection and rotatory angle of the ith column are

$$\{u \ w \ \psi\}_i^*(x_i, t) = \{U \ W \ \Psi\}_i^*(x_i)\sin(\omega t) \tag{10a}$$

which can be obtained by replacing the constants B_{1i} - B_{6i}, p_1, p_2 and functions U_i, W_i, Ψ_i, β_1 and β_2 of Eqs. (8)-(9d) with the constants B_{1i}^* - B_{6i}^*, p_1^*, p_2^* and functions U_i^*, W_i^*, Ψ_i^*, β_1^* and β_2^*. The corresponding axial force, transverse shear force and moment of the column are denoted as

$$\{n \ q \ m\}_i^*(x_i, t) = \{N \ Q \ M\}_i^*(x_i)\sin(\omega t) \tag{10b}$$

Substituting the functions $U_i(x)$, $W_i(x)$, $\Psi_i(x)$, $N_i(x)$, $Q_i(x)$ and $M_i(x)$. into Eq. (3) and arranging the results into the symbolic vector forms yield

$$\{U \ W \ \Psi N \ Q \ M\}_{ia}^T = [P]_i\{B_1 B_2 B_3 B_4 B_5 B_6\}_i^T \tag{11a}$$

$$\{U \ W \ \Psi N \ Q \ M\}_{ib}^{T} = [G \ ]_i \{B_1 B_2 B_3 B_4 B_5 B_6\}_i^{T} \tag{11b}$$

The relation of displacements and forces at both ends of the ith beam is therefore obtained to be of the form

$$\{U \ W \ \Psi N \ Q \ M\}_{ib}^{T} = [R \ ]_i \{U \ W \ \Psi N \ Q \ M\}_{ia}^{T} \tag{12}$$

where $[R]_i = [G]_i[P]_i^{-1}$. Similarly, the following relation

$$\{U \ W \ \Psi N \ Q \ M\}_{ib}^{*T} = [R^* \ ]_i \{U \ W \ \Psi N \ Q \ M\}_{ia}^{*T} \tag{13a}$$

is obtained for the ith column. Eq. (13a) is rearranged to the vector form

$$\{-W \ U \ \Psi - Q \ N \ M\}_{ib}^{*T} = [Z^* \ ]_i \{-W \ U \ \Psi - Q \ N \ M\}_{ia}^{*T} \tag{13b}$$

By introducing these notations

$$\{D_l\}_i = \{U \ W \ \Psi\}_{ia}^{T}, \ \{D_r\}_i = \{U \ W \ \Psi\}_{ib}^{T}$$

$$\{F_l\}_i = \{N \ Q \ M\}_{ia}^{T}, \ \{F_r\}_i = \{N \ Q \ M\}_{ib}^{T} \tag{14a}$$

$$\{D_l^*\}_i = \{-W \ U \ \Psi\}_{ia}^{*T}, \ \{D_r^*\}_i = \{-W \ U \ \Psi\}_{ib}^{*T}$$

$$\{F_l^*\}_i = \{-Q \ N \ M\}_{ia}^{*T}, \ \{F_r^*\}_i = \{-Q \ N \ M\}_{ib}^{*T} \tag{14b}$$

Eqs. (12) and (13b) are organized into the vector forms

$$\begin{Bmatrix} D_r \\ F_r \end{Bmatrix}_i = \begin{bmatrix} R_{11} & R_{12} \\ R_{21} & R_{22} \end{bmatrix}_i \begin{Bmatrix} D_l \\ F_l \end{Bmatrix}_i \tag{15}$$

for the ith beam and

$$\begin{Bmatrix} D_r^* \\ F_r^* \end{Bmatrix}_i = \begin{bmatrix} Z_{11}^* & Z_{12}^* \\ Z_{21}^* & Z_{22}^* \end{bmatrix}_i \begin{Bmatrix} D_l^* \\ F_l^* \end{Bmatrix}_i \tag{16}$$

for the ith column, respectively. Employing the condition of zero displacements at the fixed bottom into Eq. (16) yields the relation of displacements and forces at the top of the column as

$$\{F_l^*\}_i = -[Z_{12}^{*-1} \ Z_{11}^* \ ]_i \ \{D_l^*\}_i \tag{17}$$

The conditions of the displacements continuity and the forces balance

$$\{D_r\}_i + \{D_l\}_{i+1} = \{D_l^*\}_{i+1} \tag{18a}$$

$$\{F_r\}_i + \{F_l\}_{i+1} + \{F_l^*\}_{i+1} = \{0 \ 0 \ 0\}^{T} \tag{18b}$$

at the junction of two adjacent beams and one connected column of the frame (see Fig. 4) imply that the relation of displacements and forces at the junction between two adjacent beams is

$$\begin{Bmatrix} D_l \\ F_l \end{Bmatrix}_{i+1} = \begin{bmatrix} I_{3 \times 3} & 0 \\ Z_{12}^{*-1} \ Z_{11}^* & -I_{3 \times 3} \end{bmatrix}_i \begin{Bmatrix} D_r \\ F_r \end{Bmatrix}_i \tag{19}$$

where is an identity matrix of order 3. Therefore, the response relation at the left junction of two adjacent beams is

$$\begin{Bmatrix} D_l \\ F_l \end{Bmatrix}_{i+1} = [S]_i \begin{Bmatrix} D_l \\ F_l \end{Bmatrix}_i \tag{20}$$

where the transfer matrix $[S]_i$ is.

$$[S]_i = \begin{bmatrix} R_{11} & R_{12} \\ R_{21} & R_{22} \end{bmatrix}_i \begin{bmatrix} I_{3\times3} & 0 \\ Z_{12}^{*-1}Z_{11}^* & -I_{3\times3} \end{bmatrix}_i$$

Under this circumstance, the response relation at both ends of the entire beam of the n-span frame is

$$\begin{Bmatrix} D_r \\ F_r \end{Bmatrix}_n = [R]_n [S]_{n-1}\cdots[S]_1 \begin{Bmatrix} D_l \\ F_l \end{Bmatrix}_1 \tag{21a}$$

or briefly expressed as

$$\begin{Bmatrix} D_r \\ F_r \end{Bmatrix}_n = \begin{bmatrix} H_{11} & H_{12} \\ H_{21} & H_{22} \end{bmatrix} \begin{Bmatrix} D_l \\ F_l \end{Bmatrix}_1 \tag{21b}$$

The zero displacement conditions at both ends of the frame imply that the jth modal frequency ω_j is determined by solving

$$[H_{12}]\{F_l\}_1 = \{0\ 0\ 0\}^T \tag{22}$$

The jth set of the mode shape functions $\{U\ W\ \Psi\}_i^{(j)}(x_i)$ of the ith beam and $\{U^*\ W^*\ \Psi^*\}_i^{(j)}(x_i)$ of the ith column are obtained by performing similar calculations described by Wang and Lin (1997a). To simplify the notations in the following section, the jth set of the mode shape functions and the corresponding set of axial force, shear force and bending moment of the entire beam of the frame are denoted, respectively, as $\{U\ W\ \Psi\}^{(j)}(x)$ and $\{N\ Q\ M\}^{(j)}(x)$ where $0\leq x\leq nL$. Furthermore, the corresponding set of axial force, shear force and bending moment of the ith column is indicated as $\{N\ Q\ M\}_i^{(j)}(x_i)$.
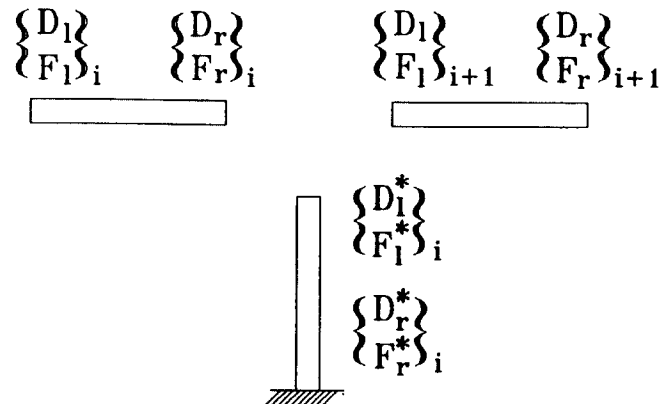

Fig. 4 Applied end forces and displacements of a typical T-type frame

4. Orthogonality of mode shape functions

The set of the *j*th mode shape functions $\{U^{(j)}\ W^{(j)}\ \Psi^{(j)}\}(x)$ of the entire beam satisfy the relations

$$-\frac{dN^{(j)}}{dx} = \omega_j^2 \rho A U^{(j)} \tag{23a}$$

$$-\frac{dQ^{(j)}}{dx} = \omega_j^2 \rho A W^{(j)} \tag{23b}$$

$$-Q^{(j)} + \frac{dM^{(j)}}{dx} = \omega_j^2 \rho I\ \Psi^{(j)} \tag{23c}$$

By omitting the description of the procedures of derivation, the following equation is obtained

$$
(\omega_j^2 - \omega_k^2) \int_0^{nL} (\rho A U^{(j)} U^{(k)} + \rho A W^{(j)} W^{(k)} + \rho I\ \Psi^{(j)} \Psi^{(k)})\,dx
$$

$$
= \sum_{i=1}^{n} \{N_{ib}^{(k)} U_{ib}^{(j)} + N_{ia}^{(k)} U_{ia}^{(j)} - U_{ib}^{(j)} U_{ib}^{(k)} - N_{ia}^{(j)} U_{ia}^{(k)}\}
$$

$$
+ \sum_{i=1}^{n} \{Q_{ib}^{(k)} W_{ib}^{(j)} + Q_{ia}^{(k)}\ W_{ia}^{(j)} - Q_{ib}^{(j)}\ W_{ib}^{(k)} - Q_{ia}^{(j)}\ W_{ia}^{(k)}\}
$$

$$
+ \sum_{i=1}^{n} \{M_{ib}^{(k)} \Psi_{ib}^{(j)} + M_{ia}^{(k)} \Psi_{ia}^{(j)} - M_{ib}^{(j)} \Psi_{ib}^{(k)} - M_{ia}^{(j)} \Psi_{ia}^{(k)}\} \tag{24}
$$

Similarly, the relation

$$
(\omega_j^2 - \omega_k^2) \sum_{i=1}^{n-1} \int_0^{L^*} \{\rho A U_i^{*(j)} U_i^{*(k)} + \rho A W_k^{*(j)} W_i^{*(k)} + \rho I\ \Psi_i^{*(j)} \Psi_i^{*(k)}\}
$$

$$
= \sum_{i=1}^{n-1} \{N_{ib}^{*(k)} U_{ib}^{*(j)} + N_{ia}^{*(k)} U_{ia}^{*(j)} - U_{ib}^{*(j)} U_{ib}^{*(k)} - N_{ia}^{*(j)} U_{ia}^{*(k)}\}
$$

$$
= \sum_{i=1}^{n-1} \{Q_{ib}^{*(k)}\ W_{ib}^{*(j)} + Q_{ia}^{*(k)}\ W_{ia}^{*(j)} - Q_{ib}^{*(j)}\ W_{ib}^{*(k)} - Q_{ia}^{*(j)}\ W_{ia}^{*(k)}\}
$$

$$
= \sum_{i=1}^{n-1} \{M_{ib}^{*(k)} \Psi_{ib}^{*(j)} + M_{ia}^{*(k)}\ \Psi_{ia}^{*(j)} - M_{ib}^{*(j)}\ \Psi_{ib}^{*(k)} - M_{ia}^{*(j)}\ \Psi_{ia}^{*(k)}\} \tag{25}
$$

is obtained for all columns. Performing the summation of Eqs. (24) and (25) yields the orthogonality of any two distinct sets of the mode shape functions

$$
\int_0^{nL} (\rho A U^{(j)} U^{(k)} + \rho A W^{(j)} W^{(k)} + \rho I\ \Psi^{(j)} \Psi^{(k)})\,dx
$$

$$
+ \sum_{i=1}^{n-1} \int_0^{L^*} (\rho A U_i^{*(j)} U_i^{*(k)} + \rho A W_i^{*(j)} W_i^{*(k)} + \rho I\ \Psi_i^{*(j)} \Psi_i^{*(k)})\,dx_i = 0,\ j \neq k \tag{26a}
$$

which also implies

$$
\int_0^{nL} \left(U^{(j)} \frac{dN^{(k)}}{dx} + W^{(j)} \frac{dQ^{(k)}}{dx} + \Psi^{(j)} \left(Q^{(k)} - \frac{dM^{(k)}}{dx} \right) \right) dx
$$

$$+ \sum_{i=1}^{n-1} \int_0^{L^*} \left(U_i^{*(j)} \frac{dN_i^{*(k)}}{dx_i} + W_i^{*(j)} \frac{dQ_i^{*(k)}}{dx_i} + \rho I \, \Psi_i^{*(j)} \left(Q_i^{*(k)} - \frac{dM_i^{*(k)}}{dx_i} \right) \right) dx_i = 0 \, , \; j \neq k \quad (26b)$$

5. Forced vibration

According to the orthogonality of two distinct sets of the mode shape functions, the superposition method is adopted in the section to study the frame's forced vibration. The respective longitudinal displacement, transverse deflection and rotatory angle of the entire beam are

$$\{u \; w \; \psi\}(x,t) = \sum_{j=1} a_j(t) \{U \; W \; \Psi\}^{(j)}(x) \quad (27)$$

Moreover, the longitudinal displacement, transverse deflection and rotatory angle of the *i*th column, respectively, are

$$\{u \; w \; \psi\}_i^*(x_i,t) = \sum_{j=1} a_j(t) \{U \; W \; \Psi\}_i^{*(j)}(x_i) \quad (28)$$

Under this circumstance, the governing equations are

$$-\sum_{j=1} a_j(t) \frac{dN^{(j)}}{dx} + \sum_{j=1} \rho A U^{(j)} \frac{d^2 a_j}{dt^2} = 0 \quad (29a)$$

$$-\sum_{j=1} a_j \frac{dQ^{(j)}}{dx} + \sum_{j=1} \rho A W^{(j)} \frac{d^2 a_j}{dt^2} = F(x,t) \quad (29b)$$

$$-\sum_{j=1} a_j \left(Q^{(j)} - \frac{dM^{(j)}}{dx} \right) + \sum_{j=1} \rho I \, \Psi^{(j)} \frac{d^2 a_j}{dt^2} = 0 \quad (29c)$$

for the entire beam and

$$-\sum_{j=1} a_j(t) \frac{dN_i^{*(j)}}{dx_i} + \sum_{j=1} \rho A U_i^{*(j)} \frac{d^2 a_j}{dt^2} = 0 \quad (30a)$$

$$-\sum_{j=1} a_j \frac{dQ_i^{*(j)}}{dx_i} + \sum_{j=1} \rho A W_i^{*(j)} \frac{d^2 a_j}{dt^2} = 0 \quad (30b)$$

$$-\sum_{j=1} a_j \left(Q_i^{*(j)} - \frac{dM_i^{*(j)}}{dx_i} \right) + \sum_{j=1} \rho I \, \Psi_i^{*(j)} \frac{d^2 a_j}{dt^2} = 0 \quad (30c)$$

for the *i*th column. By adopting the relation of orthogonality (26a, b), Eqs. (29a)-(30c) are combined to yield the governing equation of the *k*th modal amplitude a_k

$$\frac{d^2 a_k}{dt^2} + \omega_k^2 a_k = g_k(t) \quad (31)$$

in which the kth modal frequency ω_k and the corresponding excitation $g_k(t)$ are

$$\omega_k^2 = m_k/s_k \, , \, g_k(t) = \int_0^{nL} F(x,t) W^{(k)}(x) \, dx/s_k \tag{32}$$

where m_k and s_k are the respective modal mass and stiffness:

$$s_k = \int_0^{nL} (\rho A U^{(k)} U^{(k)} + \rho A W^{(k)} W^{(k)} + \rho I \, \Psi^{(k)} \Psi^{(k)}) \, dx$$

$$+ \sum_{i=1}^{n-1} \int_0^{L^*} (\rho A U_i^{*(k)} U_i^{*(k)} + \rho A W_i^{*(k)} W_i^{*(k)} + \rho I \, \Psi_i^{*(k)} \Psi_i^{*(k)}) \, dx_i \tag{33}$$

$$m_k = - \int_0^{nL} \left(U^{(k)} \frac{dN^{(k)}}{dx} + W^{(k)} \frac{dQ^{(k)}}{dx} + \Psi^{(k)} \left(Q^{(k)} - \frac{dM^{(k)}}{dx} \right) \right) dx$$

$$- \sum_{i=1}^{n-1} \int_0^{L^*} \left(U_i^{*(k)} \frac{dN_i^{*(k)}}{dx_i} + W_i^{*(k)} \frac{dQ_i^{*(k)}}{dx_i} + \Psi_i^{*(k)} \left(Q_i^{*(k)} - \frac{dM_i^{*(k)}}{dx_i} \right) \right) dx_i \tag{34}$$

For the values of initial conditions of the frame being zeros, the history of the kth modal amplitude $a_k(t)$ is

$$a_k(t) = \int_0^t h_k(t-\tau) g_k(\tau) \, d\tau \tag{35}$$

The impulse response $h_k(\tau)$ of Eq. (35) is

$$h_k(\tau) = \begin{cases} \sin(\omega_k \tau)/\omega_k & (0 < \tau) \\ 0 & (\tau \le 0) \end{cases} \tag{36}$$

6. Motion of a random load on the frame

Fig. 5 depicts that a load $F(t)$ moves on the frame at a constant velocity v. This load is a random process with a constant mean value $F_0(=\,<F(t)>)$ and a centered deviation $f(t)$. The covariance $C_f(t_1, t_2)$ between $F(t_1)$ and $F(t_2)$ is

$$C_f(t_1, t_2) = <f(t_1) f(t_2)> \tag{37}$$

in which $<\,>$ is the operator of mean value. The respective histories of the kth modal excitation $g_k(t)$ and its corresponding mean value $<g_k(t)>$, and the covariance $C_{gjgk}(t_1, t_2)$ between $g_j(t_1)$ and $g_k(t_2)$ are

1) $0 \le t, t_1, t_2 \le nL/v$

$$g_k(t) = F(t) W^{(k)}(vt)/s_k \tag{38a}$$

$$<g_k(t)> = F_0 W^{(k)}(vt)/s_k \tag{38b}$$

$$C_{gjgk}(t_1, t_2) = C_f(t_1, t_2) W^{(j)}(vt_1) W^{(k)}(vt_2)/s_j s_k \tag{38c}$$

2) $nL/v < t, t_1$ (or t_2)

$$g_k(t) = 0 \tag{39a}$$

$$<g_k(t)> = 0 \tag{39b}$$

$$C_{g_j g_k}(t_1, t_2) = 0 \tag{39c}$$

The respective mean value histories of the *j*th modal amplitude, transverse deflection and moment of the entire beam are

$$<a_j(t)> = \int_{-\infty}^{\infty} h_j(\tau) <g_j(t-\tau)> d\tau \tag{40a}$$

$$<w(x,t)> = \sum_{j=1}^{\infty} W^{(j)}(x) <a_j(t)> \tag{40b}$$

$$<m(x,t)> = \sum_{j=1}^{\infty} M^{(j)}(x) <a_j(t)> \tag{40c}$$

The covariance $C_{a_j a_l}(t_1, t_2)$ between $a_j(t_1)$ and $a_l(t_2)$ is

$$C_{a_j a_l}(t_1, t_2) = \int_{-\infty}^{\infty} h_j(t_1 - \tau_1) h_l(t_2 - \tau_2) C_{g_j g_l}(\tau_1, \tau_2) d\tau_1 d\tau_2 \tag{40d}$$

The deflection covariance $C_w(x_1, x_2, t_1, t_2)$ between $w(x_1, t_1)$ and $w(x_2, t_2)$ is

$$C_w(x_1, x_2, t_i, t_2) = \sum_{j=1}^{\infty} \sum_{l=1}^{\infty} W^{(j)}(x_1) W^{(l)}(x_2) C_{a_j a_l}(t_1, t_2) \tag{41a}$$

Moreover, the moment covariance $C_m(x_1, x_2, t_1, t_2)$ between $m(x_1, t_1)$ and $m(x_2, t_2)$, is

$$C_m(x_1, x_2, t_1, t_2) = \sum_{j=1}^{\infty} \sum_{l=1}^{\infty} M^{(j)}(x_1) M^{(l)}(x_2) C_{a_j a_l}(t_1, t_2) \tag{41b}$$

Consider the centered deviation $f(t)$ to be a stationary process, i.e.,

$$C_f(t_1, t_2) = C_f(t_1 - t_2) \tag{42}$$

The covariance $C_{g_j g_l}(t_1, t_2)$ and the covariance $C_{a_j a_l}(t_1, t_2)$, respectively, are

$$C_{g_j g_l}(t_1, t_2) = \begin{cases} C_f(t_1 - t_2) W^{(j)}(vt_1) W^{(l)}(vt_2)/(s_j s_l), & 0 \le t_1, t_2 \le nL/v \\ 0, & nL/v \le t_1, t_2 \end{cases} \tag{43a}$$
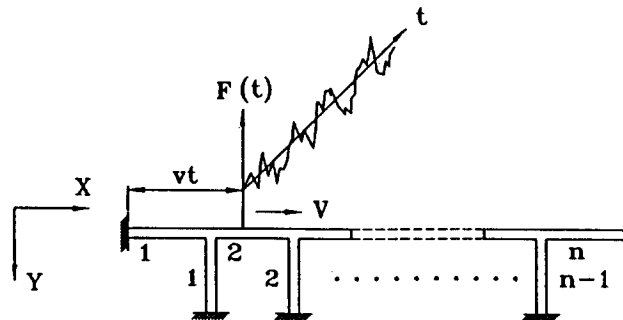

Fig. 5 A concentrated load traversing on the *n*-span Timoshenko frame at a constant velocity

$$C_{a_j a_l}(t_1, t_2) = \int_{-\infty}^{\infty} \int_{-\infty}^{\infty} h_j(t_1 - \tau_1) h_l(t_2 - \tau_2) C_{g_j g_k}(\tau_1, \tau_2) d\tau_1 d\tau_2 / s_j s_l \qquad (43b)$$

Moreover, the variances of deflection and moment of the entire beam are denoted as $\sigma_w^2(x, t)$ and $\sigma_m^2(x, t)$, respectively, which are

$$\sigma_w^2(x, t) = C_w(x, x, t, t) = \sum_{j=1} \sum_{l=1} W^{(j)}(x) W^{(l)}(x) C_{a_j a_l}(t, t) \qquad (44a)$$

$$\sigma_m^2(x, t) = C_m(x, x, t, t) = \sum_{j=1} \sum_{l=1} M^{(j)}(x) M^{(l)}(x) C_{a_j a_l}(t, t) \qquad (44b)$$

The following two typical types of variances with the spectral density S_0 are considered (Figs. 6(a) and 6(b)) in the study:

(1) White Noise

$$C_f(\tau) = S_0^2 \delta(\tau) \qquad (45a)$$

(2) Cosine

$$C_f(\tau) = S_0^2 \cos(\omega_0 \tau) \qquad (45b)$$

7. Illustrative examples and discussion

To illustrate the numerical result in this study, the non-dimensional variables are introduced as follows;

$$\bar{u} = u/L, \quad \bar{w} = w/\eta, \quad \bar{\psi} = \psi L/\eta, \quad \bar{x} = x/L, \quad \bar{t} = (EL/\rho AL^4)^{1/2} t,$$
$$\bar{p} = p/EA, \quad \bar{q} = qL^3/EI\eta, \quad \bar{m} = mL^2/EI\eta, \quad r = \eta/L, \quad l_r = L^*/L,$$
$$\bar{\omega} = (\rho AL^4/EI)^{1/2}\omega, \quad \bar{F}_0 = F_0 L^4/EI\eta, \quad \bar{S}_0 = S_0 L^4/EI\eta$$

where l_r is the length ratio of column to one span. Moreover, Poisson's ratio $\mu = 1/3$, the shear coefficient $\kappa = 2/3$ of each branch and $r = 0.03$ are considered in this section. The value of $\bar{F}_0$ is assumed to be unity. The following parameters are defined to illustrate the numerical results,
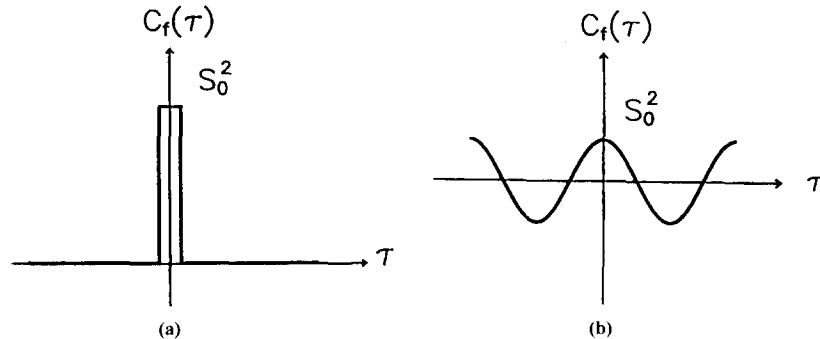first modal frequency of Timoshenko frame, $\bar{\omega}_1$;

$$C_f(T) \qquad\qquad\qquad C_f(T)$$

$$S_0^2 \qquad\qquad\qquad\qquad S_0^2$$

(a)   (b)

Fig. 6 Two types of variances: (a) white noise process and (b) cosine process

velocity ratio, $\alpha(= 100v / (E/\rho)^{1/2})$;

maximum $<\underline{w}>$ of the entire beam during the motion of load, $<\overline{W}>_{max}$;

maximum $<\underline{m}>$ of the entire beam during the motion of load, $<\overline{M}>_{max}$;

maximum deflection variance of the entire beam during the motion of load, $\overline{\sigma}_{W, max}$;

maximum moment variance of the entire beam during the motion of load, $\overline{\sigma}_{M, max}$;

position of $\overline{\sigma}_{W, max}$ during the motion of load, $(\overline{X}_W)_\sigma$;

position of $\overline{\sigma}_{M, max}$ during the motion of load, $(\overline{X}_M)_\sigma$;

velocity at which $\leq \overline{W}>_{max}$ appears, α_c;

velocity at which $\overline{\sigma}_{W, max}$ appears, α_σ;

The lowest sixteen modal frequencies and their corresponding mode shape functions of frames are sufficient (Wang and Lin 1997b) to be considered in the study. Furthermore, the velocity range to be considered is $0 \leq \alpha \leq 16$.

7.1. Mean value

Figs. 7(a) and 7(b) depict the comparisons of two frame models on the $<\overline{W}>_{max}$-α distribution and the $<\overline{M}>_{max}$-α distribution of a three-span frame $(l_r = 1)$. The effect of shear deformation causes the Timoshenko frame to have a greater $<\overline{W}>_{max}$ than Bernoulli-Euler frame's within the low velocity range $0 \leq \alpha \leq 9$. The first modal frequency is the most dominant factor on a frame's vibration. The first modal frequency of Bernoulli-Euler frame is larger than that of Timoshenko frame. According to this result, the lowest bending wave phase velocity in Bernoulli-Euler frame is greater than that in Timoshenko frame. The α_c of Bernoulli-Euler frame is, consequently, greater than that of Timoshenko frame. Within the low velocity range $0 \leq \alpha \leq 5$, the load can be regarded as a quasi-static load. The effect of rotatory inertia on reducing the moment of the frame is negligible within this velocity range. Therefore, the $<\overline{M}>_{max}$ difference between these two frames is slight within the low velocity range. However, the effect of rotatory inertia on their $<\overline{M}>_{max}$ differences cannot be neglected for being greater than 5. The largest $<\overline{M}>_{max}$ difference appears at α_c.

Figs. 8(a) and 8(b) compare three l_r values on the $<\overline{W}>_{max}$-α distribution and the $<\overline{M}>_{max}$-α distribution of a three-span Timoshenko frame, respectively. The shorter column length causes a

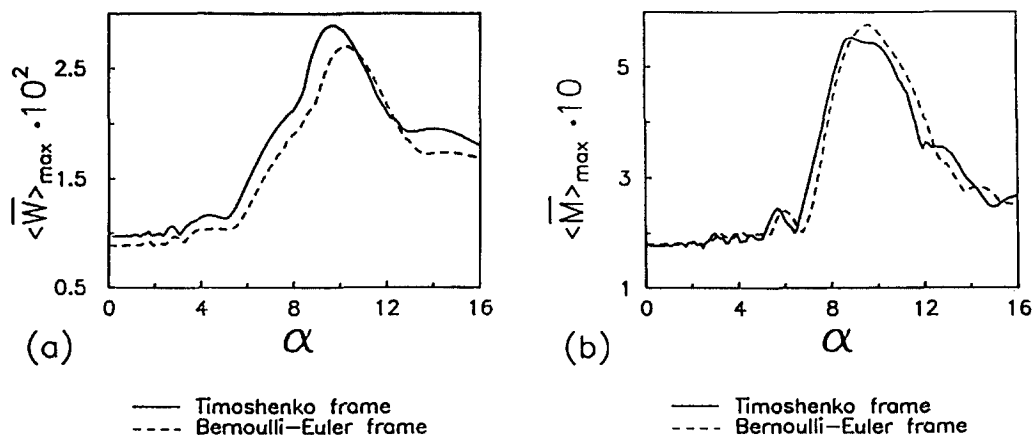Fig. 7 Comparisons of two frame models on (a) the $<\overline{W}>_{max}$-α distribution and (b) the $<\overline{M}>_{max}$-α distribution of a three-span frame $(r = 0.03, l_r = 1)$ due to a random load
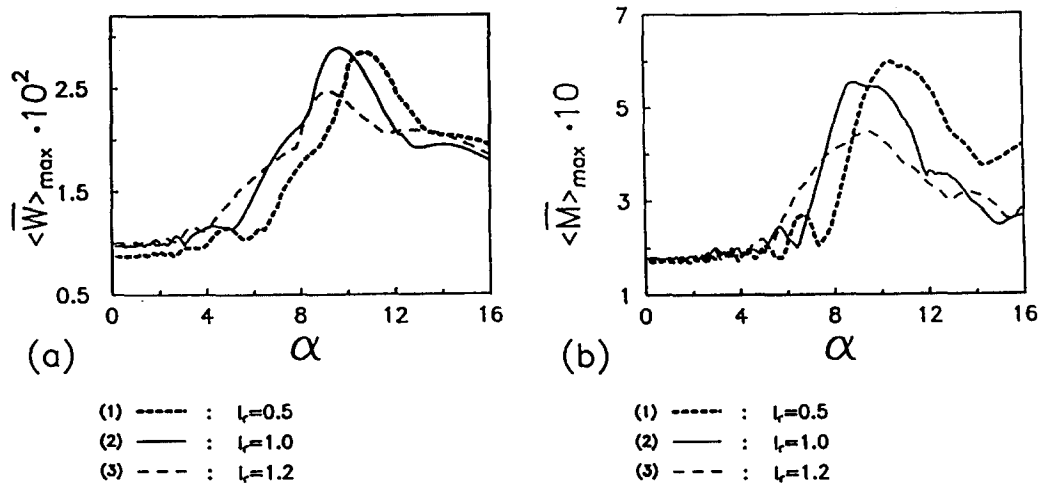
(1) $\bullet\bullet\bullet\bullet\bullet$: $l_r{=}0.5$

(2) ——— : $l_r{=}1.0$

(3) – – – : $l_r{=}1.2$

(1) $\bullet\bullet\bullet\bullet\bullet$: $l_r{=}0.5$

(2) ——— : $l_r{=}1.0$

(3) – – – : $l_r{=}1.2$

Fig. 8 Comparisons of three l_r values on (a) the $<\overline{W}>_{max}$-α distribution and (b) $<\overline{M}>_{max}$-α distrbution of a three-span Timoshenko frame ($r = 0.03$) due to a random load

greater $\overline{\omega}_1$. The shorter the column and the greater $\overline{\omega}_1$ implies that a shorter column induces a more stiff frame. As this result indicates, the shorter column causes both less $<\overline{W}>_{max}$ and $<\overline{M}>_{max}$ within a low velocity range. Fig. 8(a) reveals that the frame with shorter columns has a larger α_c.

Figs. 9(a) and 9(b) display the effects of span number on the $<\overline{W}>_{max}$-α distribution and the $<\overline{M}>_{max}$-α distribution of a multispan Timoshenko frame ($l_r = 1$), respectively. The effect of bending wave dominating the vibration of frame is more apparent for a higher span number. Therefore, the higher the span number implies the more both $<\overline{W}>_{max}$ and $<\overline{M}>_{max}$ are constrained within the neighborhood of the critical velocity. Furthermore, the higher the span number of frame implies the closer α_c to the lowest phase velocity of bending wave is in the structure.
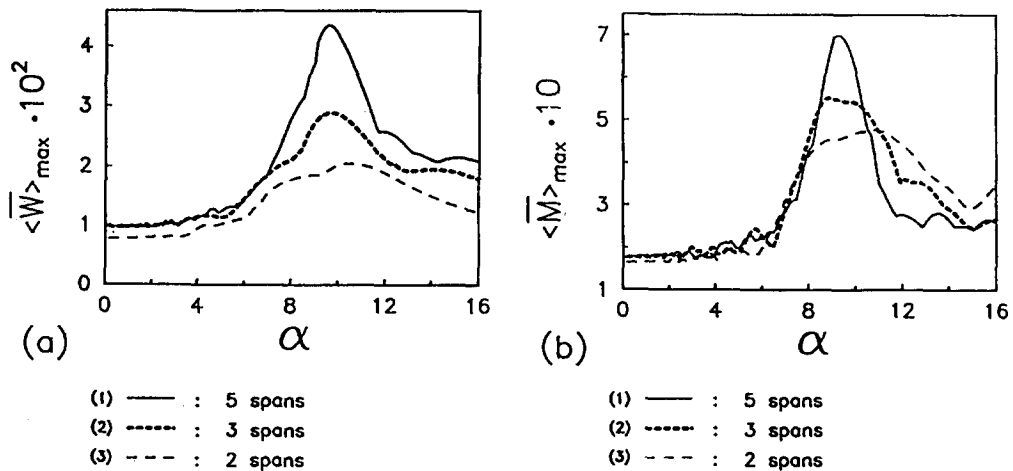

(1) ——— : 5 spans

(2) $\bullet\bullet\bullet\bullet\bullet$: 3 spans

(3) – – – : 2 spans

(1) ——— : 5 spans

(2) $\bullet\bullet\bullet\bullet\bullet$: 3 spans

(3) – – – : 2 spans

Fig. 9 Span number effects on (a) the $<\overline{W}>_{max}$-α distribution and (b) the $<\overline{M}>_{max}$-α distribution of a multispan Timoshenko frame ($r = 0.03$, $l_r = 1$) due to a random load

7.2. White noise

The frequency domain of power spectrum of a white noise variance ranges from negative infinite to positive infinite. Theoretically, all modes of the frame should be excited. However, the magnitude of each modal amplitude depends on the loading time. A slow moving load induces a longer duration of forced vibration. The frame is in the resonance with load at $\alpha = 0$. However, the load moves too fast to excite all modal responses at a high velocity ratio. Therefore, Figs. 10(a) and 10(b) reveal that both $\sigma_{W,\,max}$ and $\sigma_{M,\,max}$ are infinite at $\alpha = 0$ and exponentially decrease to certain values as α increases. The higher the number of span implies a longer duration of forced vibration of the frame due to the moving load. The longer duration of forced vibration induces the higher the number of excited mode. Therefore, the higher the number of span causes a larger $\sigma_{W,\,max}$, as indicated in Fig. 10(a). The number of
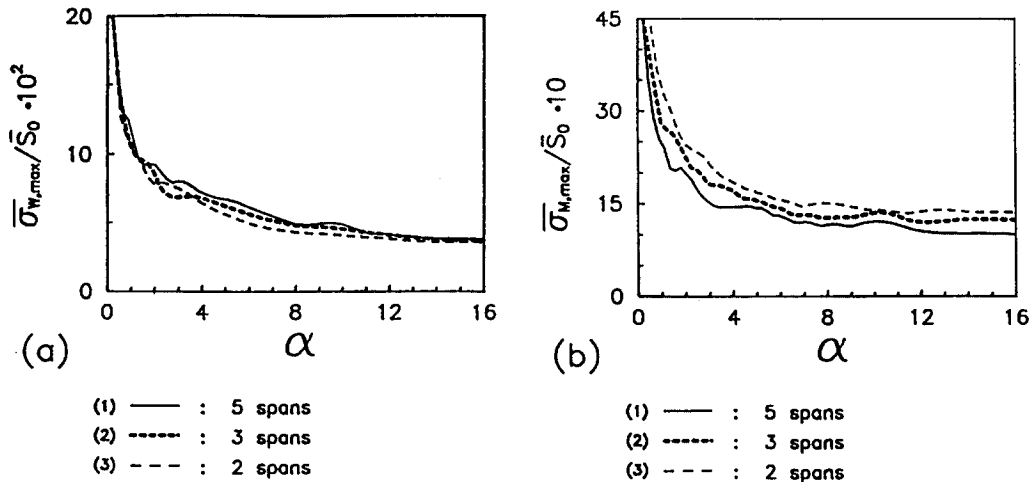

(1) ——— : 5 spans   (1) ——— : 5 spans
(2) ••••• : 3 spans   (2) ••••• : 3 spans
(3) – – – : 2 spans   (3) – – – : 2 spans

Fig. 10 Span number effects on (a) the $\overline{\sigma}_{W,\,max}$ distribution and (b) the $\overline{\sigma}_{M,\,max}$ distribution of a multispan Timoshenko frame ($r = 0.03$, $l_r = 1$) due to a random load with white noise variance
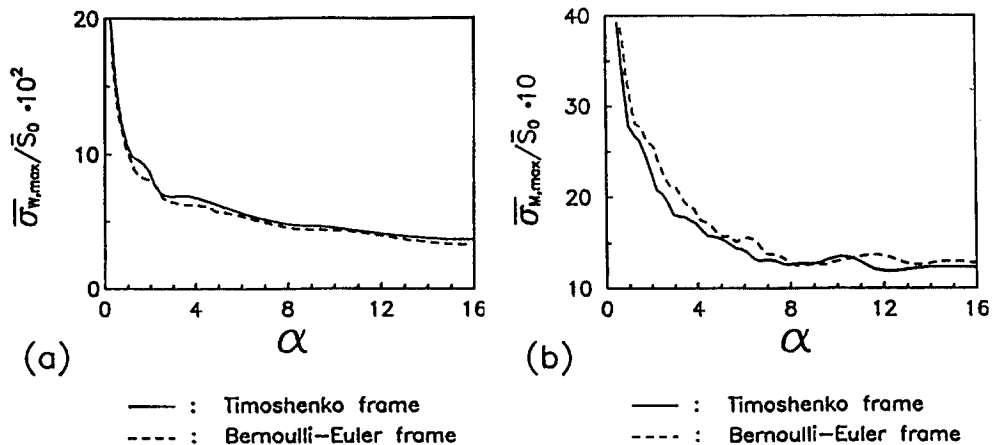

——— : Timoshenko frame   ——— : Timoshenko frame
– – – : Bernoulli–Euler frame   – – – : Bernoulli–Euler frame

Fig. 11 Comparisons of two frame models on (a) the $\overline{\sigma}_{W,\,max}$-$\alpha$ distribution and (b) $\overline{\sigma}_{M,\,max}$-$\alpha$ the distribution of a three-span frame ($r = 0.03$, $l_r = 1$) due to a random load with white noise variance

column support increases as the number of span increases. Each column support produces a countered moment on the beam. Therefore, the higher the number of span implies the higher the number of countered moment. Consequently, Fig. 10(b) reveals that for any value of α as the span number increases the $\overline{\sigma}_{M,\ max}$ decreases.

Figs. 11(a) and 11(b) compare two frame models on the $\overline{\sigma}_{W,\ max}$-$\alpha$ distribution and the $\overline{\sigma}_{M,\ max}$-$\alpha$ distribution of a three-span frame ($l_r = 1$) due to the load with a white noise variance, respectively. Fig. 11(a) reveals that the shear deformation enlarges the $\overline{\sigma}_{W,\ max}$ of frame. However, Fig. 11(b) indicates that the rotatory inertia reduces the $\overline{\sigma}_{M,\ max}$ of frame.

Three l_r values on the $\overline{\sigma}_{W,\ max}$-$\alpha$ distribution and the $\overline{\sigma}_{M,\ max}$-$\alpha$ distribution of a three-span Timoshenko frame are compared in Figs. 12(a) and 12(b), respectively. The smaller l_r value implies the smaller mass of a frame. Therefore, both $\overline{\sigma}_{W,\ max}$ and $\overline{\sigma}_{M,\ max}$ are larger for a smaller l_r value. Fig. 13(a) shows that the $\overline{\sigma}_{W,\ max}$ always appears at the middle of the second span which has more flexibility than the others. The fixed ends always have the maximum countered moment as displayed in Fig. 13(b).
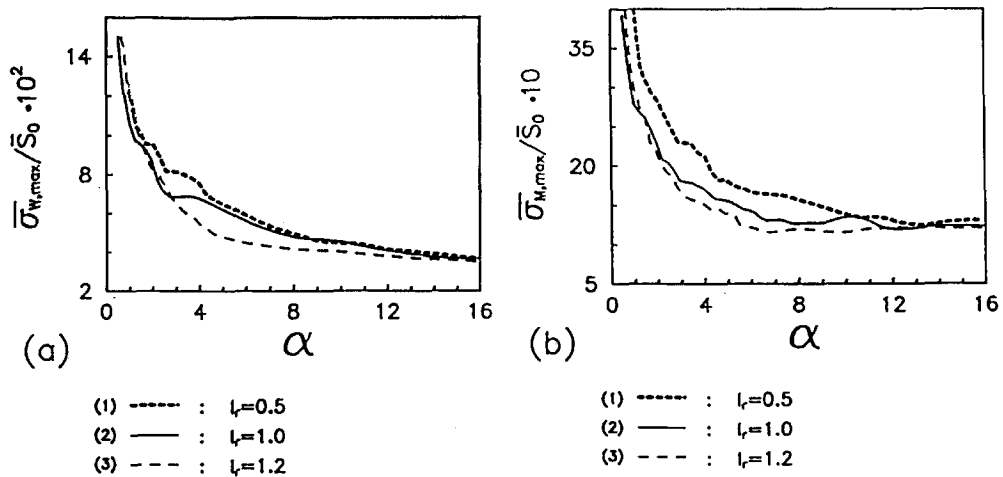

(1) — — — : l_r=0.5
(2) ——— : l_r=1.0
(3) - - - : l_r=1.2

(1) — — — : l_r=0.5
(2) ——— : l_r=1.0
(3) - - - : l_r=1.2

Fig. 12 Comparisons of three, l_r values on (a) the $\overline{\sigma}_{W,max}$-$\alpha$ distribution and (b) the $\overline{\sigma}_{M,max}$-$\alpha$ distribution of a three- span Timoshenko frame ($r = 0.03$) due to a random load with white noise variance
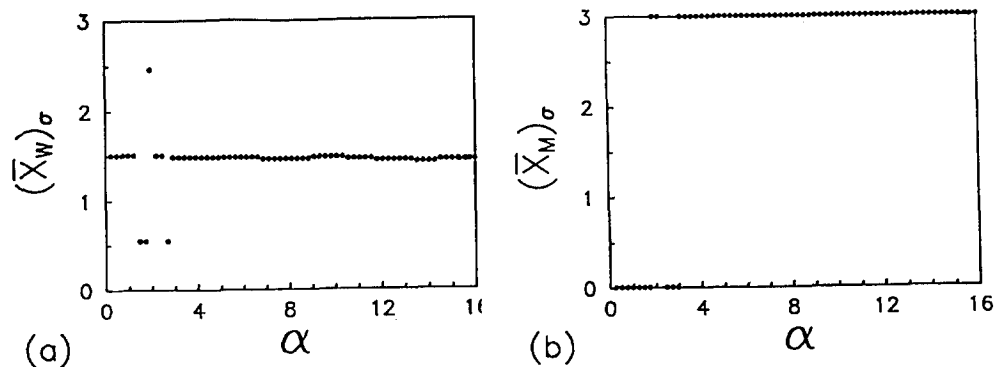

Fig. 13 (a) The $(\overline{X}_W)_\sigma$-α distribution and (b) the $(\overline{X}_M)_\sigma$-α distribution of a three-span Timoshenko frame ($r = 0.03$, $l_r = 1$) due to a random load with white noise variance

7.3. Cosine process

The data $l_r = 1$ of a three-span frame is considered to study the velocity effect and the frequency effect of load on the response variances of the structure. Figs. 14(a) and 14(b) depict that the comparisons of three $\bar{\omega}_0(= 0.5\bar{\omega}_1,\ 0.8\bar{\omega}_1,\ \bar{\omega}_1)$ values on the $\bar{\sigma}_{W,\ max}$-α distribution and the $\bar{\sigma}_{M,\ max}$-α distribution of a three-span Timoshenko frame, respectively, due to the moving load with a variance of cosine wave. Both figures reveal that the larger $\bar{\omega}_0$ of the variance has the smaller α_σ of the frame. The smaller α_σ implies a longer duration of load on the frame. Therefore, the larger $\bar{\omega}_0$ causes both the higher $\bar{\sigma}_{W,\ max}$ and $\bar{\sigma}_{M,\ max}$. The moving load can be regarded as a steady state loading on the frame as α approaches zero. The frame will be consequently in a resonant state for $\bar{\omega}_0$ being the first modal frequency of the structure at $\alpha = 0$. The similar phenomenon occurs in a beam caused by a moving random force (Fry'ba 1976). The duration of forced vibration
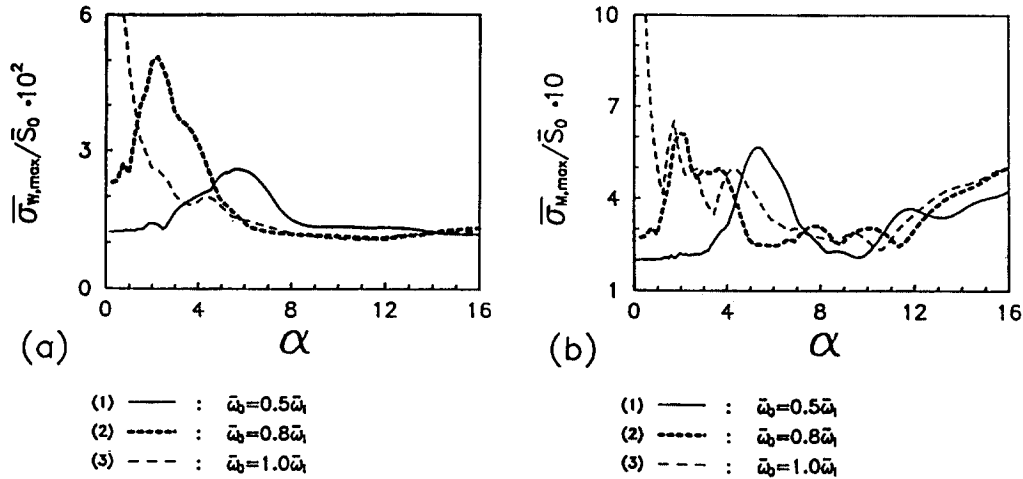
Fig. 14 Comparisons of three $\bar{\omega}_0$ values of cosine variance on (a) the $\bar{\sigma}_{W,\ max}$-α distribution and (b) the $\bar{\sigma}_{M,\ max}$-α distribution of a three-span Timoshenko frame $(r = 0.03,\ l_r = 1)$
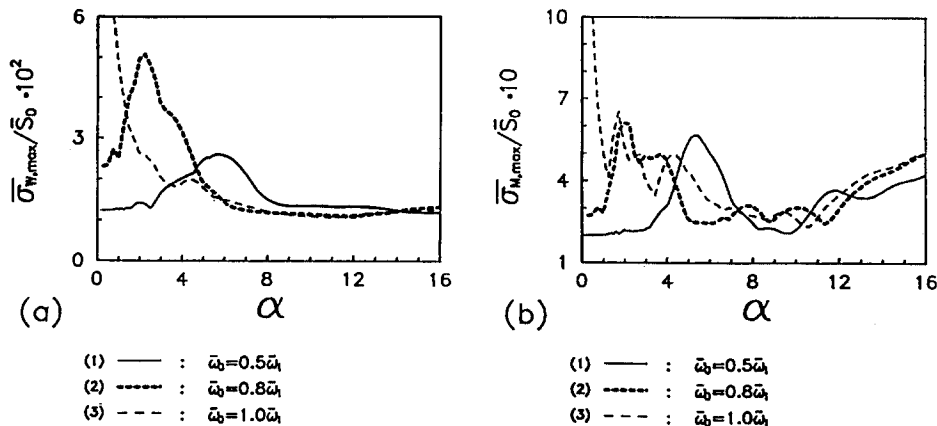
Fig. 15 Comparisons of two frame models on (a) the $\bar{\sigma}_{W,\ max}$-α distribution and (b) the $\bar{\sigma}_{M,\ max}$-α distribution of a three-span frame $(r = 0.03,\ l_r = 1)$ due to a load with cosine variance $(\bar{\omega}_0 = 0.5\bar{\omega}_1)$
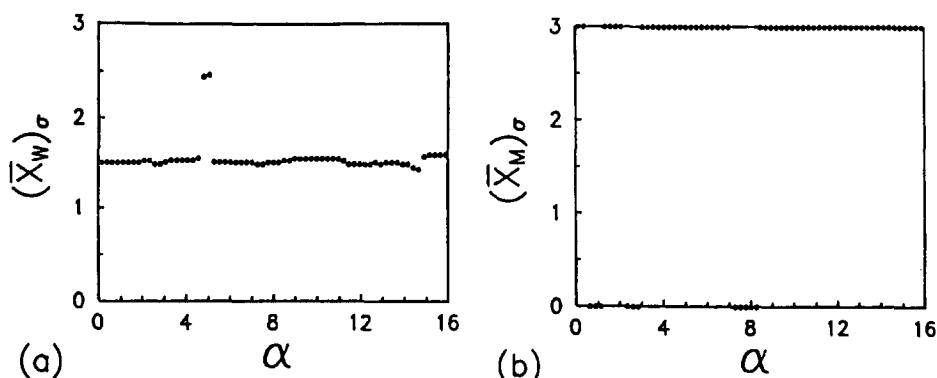
Fig. 16 (a) The $(\overline{X}_W)_\sigma$-α distribution and (b) the $(\overline{X}_M)_\sigma$-α distribution of a three-span Timoshenko frame ($r = 0.03$, $l_r = 1$) due to a load with cosine variance ($\overline{\omega}_0 = 0.5\overline{\omega}_1$)

decreases as α increases. A short duration of forced vibration implies that the value of cosine function will be independent of $\overline{\omega}_0$ at a high α. Under this circumstance, the cosine variance can be regarded as a constant variance at a high . This reason accounts for why the difference between these three $\overline{\sigma}_{W, max}$, as indicated in Fig. 14(a), is slight for $\alpha \geq 13$. Furthermore, the less frequency difference of variance implies a less $\overline{\sigma}_{M, max}$ difference for $\alpha \geq 13$.

Figs. 15(a) and 15(b) compare two frame models on the $\overline{\sigma}_{W, max}$-$\alpha$ distribution and the $\overline{\sigma}_{M, max}$-$\alpha$ distribution of a three-span frame due to the load with a cosine variance ($\overline{\omega}_0 = 0.5\overline{\omega}_1$), respectively. The first modal frequency of Timoshenko frame is less than that of the Bernoulli-Euler frame. Therefore, $\overline{\omega}_0$ is closer to the first modal frequency of Timoshenko frame than that of Bernoulli-Euler frame. According to this reason, both absolute $\overline{\sigma}_{W, max}$ and $\overline{\sigma}_{M, max}$ of Timoshenko frame are greater than those of Bernoulli-Euler frame. However, of Timoshenko frame is less than that of Bernoulli-Euler frame. Both Figs. 14(a) and 15(a) or Figs. 14(b) and 15(b) reveal that the load's velocity effect on the tendency of $\overline{\sigma}_{W, max}$-$\alpha$ or $\overline{\sigma}_{M, max}$-$\alpha$ distribution of the Timoshenko frame is similar.

Fig. 16(a) reveals that the $\overline{\sigma}_{W, max}$ of Timoshenko frame due to a cosine variance ($\overline{\omega}_0 = 0.5\overline{\omega}_1$) always appears at the middle of the second span. The $\overline{\sigma}_{M, max}$ due to the same load occurs at the fixed ends, as indicated in Fig. 16(b).

8. Conclusions

A multispan Timoshenko frame subjected to a moving random load is investigated analytically in this paper. Results reveal that both maximum mean value and maximum variance of transverse deflection always appear at the center of the middle span of the entire beam. In addition, results also indicate that both maximum mean value and maximum variance of moment always occur at one fixed end of the entire beam. The absolute maximum mean value of transverse deflection occurs at the critical velocity. Both the maximum variance of transverse deflection and that of moment of the entire beam due to a load with white noise process exponentially decrease for an increasing velocity. A moving load with a variance of cosine function does not induce serious deformations except at the critical velocity. Furthermore, the larger frequency of the process implies a smaller critical

velocity.

Acknowledgements

References

Blejwas, T.E., Feng, C.C. and Ayre, R.S. (1979), "Dynamic interaction of moving vehicles and structures", *Journal of Sound and Vibration,* **67**(4), 513-521.

Bolotin, V.V. (1984), *Random Vibrations of Elastic Systems,* Martinus Nijhoff Publishers, The Hague.

Clough, R.W. (1955), "On the importance of higher modes of vibration in the earthquake response of a tall building", *Bulletin of the Seismological Society of America* **45**, 389-301.

Dmitriev, A.S. (1982), "Dynamics of continuous multispan beams under a moving force", *Soviet Applied Mechanics,* **18**, 179-186.

Fry'ba, L. (1971), *Vibration of Solids and Structures under Moving Loads,* Noordoff International publishing, Groningen.

Fry'ba, L. (1977), "Non-stationary response of a beam to a moving random force", *Journal of Sound and Vibration,* **46**(3), 323-338.

Iwankiewicz, R. and Sniady, P. (1984), "Vibration of a beam under random stream of moving forces", *Journal of Structural Mechanics,* **12**, 13-26.

Knowles, J.K. (1968), "On the dynamic response of a beam to a random moving load", *Journal of Applied Mechanics,* **35**(1), 1-6.

Mackertich, S. (1990), "Moving load on a Timoshenko beam", *Journal of the Acoustical Society of America,* **88**(2), 1175-1178.

Ricciardi, G. (1994), "Random vibration of beam under moving loads", *Journal of Engineering Mechanics,* **120**(11), 2361-2380.

Sniady, P. (1984), "Vibration of a beam due to a random stream of moving forces with random velocity", *Journal of Sound and Vibration,* **97**(1), 23-33.

Timoshenko, S.P. (1921), "On the correction for shear of the differential equation for transverse vibration prismatic bars", *Philosophical Magazine,* **41**, 744-746.

Wang, R.T. and Lee, S.F. (1993), "Dynamic analysis of multispan frames subjected to moving loads using the finite element method", *Journal of Civil and Hydraulic Engineering* (in Chinese), **20**(1), 7-18.

Wang, R.T. and Lin, J.S. (1997a), "Vibration of multispan frames to moving loads", *Journal of the Chinese Society of Mechanical Engineers,* **18**(2), 151-162.

Wang, R.T. and Lin, J.S. (1997b), "Vibration of T-type Timoshenko frames subjected to moving loads", *Structural Engineering and Mechanics, An International Journal,* **6**(2), 229-243.